REPORT DOCUMENTATION PAGE

Form Approved
OMB No. 0704-0188

PLEASE DO NOT RETURN YOUR FORM TO THE ABOVE ORGANIZATION.

1. REPORT DATE *(DD-MM-YYYY)*	2. REPORT TYPE	3. DATES COVERED *(From - To)*
08/01/2010	Final	10/31/2007 to 05/31/2010

4. TITLE AND SUBTITLE
'Smart' surfaces and interfaces

5a. CONTRACT NUMBER
FA9550-08-1-0007

5b. GRANT NUMBER

5c. PROGRAM ELEMENT NUMBER

6. AUTHOR(S)
John J. Moore, Ryan O'Hayre, Dan Knauss

5d. PROJECT NUMBER

5e. TASK NUMBER

5f. WORK UNIT NUMBER

7. PERFORMING ORGANIZATION NAME(S) AND ADDRESS(ES)
Colorado School of Mines,
1500 Illinois Street,
Golden,
CO 80401

8. PERFORMING ORGANIZATION REPORT NUMBER

9. SPONSORING/MONITORING AGENCY NAME(S) AND ADDRESS(ES)
AFOSR

10. SPONSOR/MONITOR'S ACRONYM(S)

11. SPONSOR/MONITOR'S REPORT NUMBER(S)
AFRL-OSR-VA-TR-2012-0051

12. DISTRIBUTION/AVAILABILITY STATEMENT
A

13. SUPPLEMENTARY NOTES

14. ABSTRACT

Abstract
A 'Smart' die coating based on AlN piezoleectric thin film sensor embedded into a tribological coating system is been investigated in this research program. Thin film sensor design and its overal incorporation within the coating system are explained briefly. Piezoelectric AlN thin film with highly preffered (002) orienattaion has been deposited by pulsed closed field unbalanced magnetron sputtering system using Cr as the electrode/adhesion layer. The effect of working pressure on residual stress and (002) orienataion of AlN thin film is discussed together with gas ratio effect on the piezoelectric measurements. Piezo-response of AlN thin films were characterized by lock-in-amplifier, which measures the output piezo-voltage of AlN thin film under cyclic loading condition using a micro-actuator.

15. SUBJECT TERMS

16. SECURITY CLASSIFICATION OF:			17. LIMITATION OF ABSTRACT	18. NUMBER OF PAGES	19a. NAME OF RESPONSIBLE PERSON
a. REPORT	b. ABSTRACT	c. THIS PAGE			19b. TELEPHONE NUMBER *(Include area code)*

Reset

FINAL REPORT TO AFOSR:
PROGRAM TITLE: "Smart Surfaces and Interfaces"
AFOSR Award Number: FA 9550-08-1-0007
CSM PROPOSAL NUMBER: 4-42820
CSM FOAPAL NUMBER: 15820-37200-1200
Principal Investigator: Dr. John J. Moore

The 'Smart Surfaces and Interfaces' research program is divided into three quite distinct research areas:

(i) The Development of 'Smart' Tribological Coatings – PI. Dr. John J. Moore
(ii) Catalyst Engineering Using Surface-Dopant Modification - PI Dr. Ryan O'Hayre
(iii) Stimuli-Responsive Polymer Brushes for Smart Surfaces and Interfaces - PI Dr. Dan Knauss

Dr. John J. Moore is the overall PI for this initiative on 'Smart' Surfaces and Interfaces. This report will be presented as three separate reports according to (i), (ii), and (iii) outlined above.

1. DEVELOPMENT OF A SMART TRIBOLOGICAL COATING

M. Hashemi, J. Lin, J.J. Moore, Advanced Coatings and Surface Engineering Laboratory, Colorado School of Mines, Golden, Colorado

Abstract

A 'Smart' die coating based on AlN piezoleectric thin film sensor embedded into a tribological coating system is been investigated in this research program. Thin film sensor design and its overal incorporation within the coating system are explained briefly. Piezoelectric AlN thin film with highly preffered (002) orienattaion has been deposited by pulsed closed field unbalanced magnetron sputtering system using Cr as the electrode/adhesion layer. The effect of working pressure on residual stress and (002) orienataion of AlN thin film is discussed together with gas ratio effect on the piezoelectric measurements. Piezo-response of AlN thin films were characterized by lock-in-amplifier, which measures the output piezo-voltage of AlN thin film under cyclic loading condition using a micro-actuator.

1. Introduction

Hard tribological coatings based on transition nitrides (e.g. CrN, CrAlN, TiAlN, etc.) and advanced nanocomposite coatings as protective layers on dies and their componenets used in Al pressure die casting have increased tool/die life, reduced machine downtime and increased thermal stability [1]. In previous research work [2-4], it has been shown that incorporating a compositionally graded and/or nanoscale multilayered structure has lead to significant improvements in hardness, wear resistance, thermal resistance and toughness of our developed coatings compared to traditional die coatings and surface treatments. In order to further improve the performance and multifunctionality of the coating system, an engineered 'smart' thin film sensor is needed to be incorporated within the die coating system.

Piezoelectric materials have been extensively used as sensors and actuators in 'smart' structures and systems. Piezoelectricity is the ability of materials to produce an electric charge in response to an applied mechanical stress or induce mechanical strain due to the application of electric field. The feasibility of using piezoelectric thin film sensors for structural integrity monitoring has been demonstrated for both metallic and composite structures used in MEMS and aeronautical structural systems [5-9]. Our goal is to embed an optimized "smart" piezoelectric layer inside our already developed tribological coating system to monitor the stress variation within the material and avoid catastrophic failure. A schematic representation of our 'smart' multifunctional tribological coating system is depicted in Fig.1. The tribological coating system containing a working layer on the top and a nanoscale multilayered or compositionally garaded intermediate layer based on Cr-Al-N coating system, will provide the combination of properties of non-wetting with liqiud aluminium, wear and oxidation resistance and improved mechanical integrity [10]. As shown in Fig.1, the piezoelecric thin film sensor is placed between the top tribological coating system and bottom of ferritic nirocarburized H13 die substrate to be able to sense the initiation of microcracking and crack propegation within the die coating or at the interface.

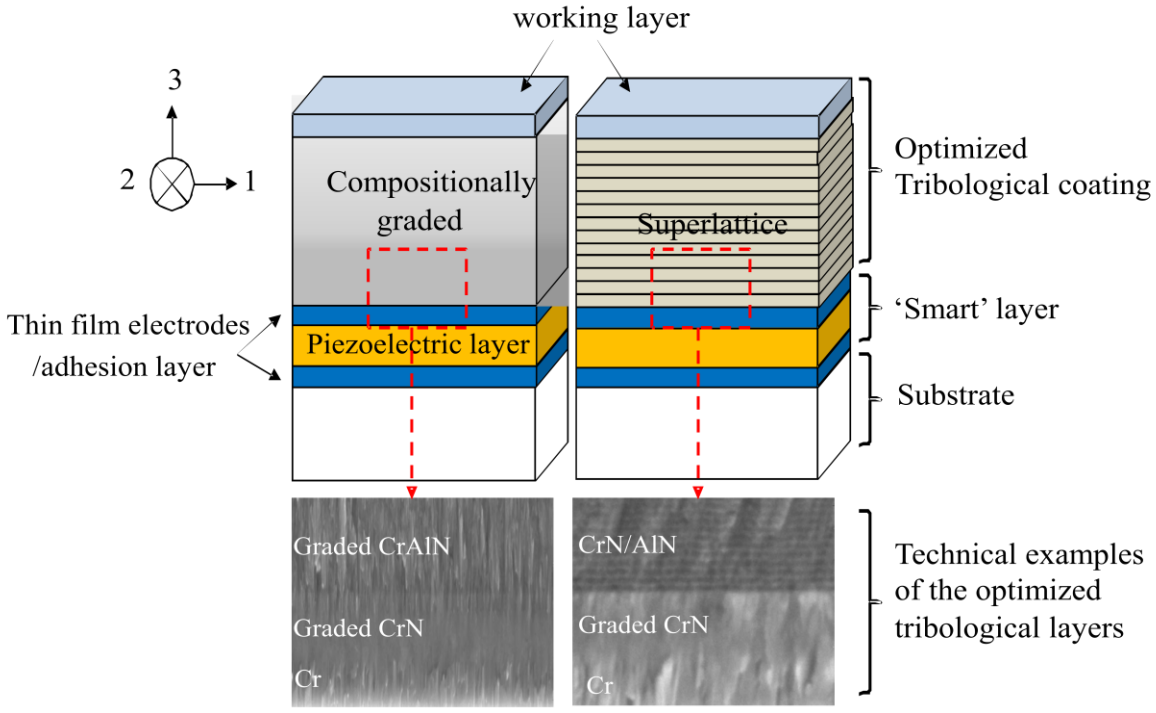

Fig.1: Schematic of Optimized Smart Multifunctional Tribological Coating System

AlN piezoelectric thin film can be used at high temperature sensor applications due to their high chemical, mechanical and piezoelectric sustainability at elevated temperatures. It is possible to detect the instantaneous stress by embedding a piezoelectric sensor within the structure. The embedded piezoelectric thin film sensor has the capability of sensing the initiation of microcracking and crack propagation by monitoring the internal stresses generated within the materials. Usually, strain in the material is increased prior to initiation of a crack and once the cracks have been generated, there is a drop in the strain level due to strain/stress relief accompanying the generation of the crack, which could be

controlled continuously by the incorporation of a smart structure in the system. The signal carrying wires, however, have to be insulated from the body as well as from each other, and that is why a high temperature non-piezoelectric insulator should coat the sensor element with the top and bottom electrodes. The reason for this requirement is to avoid charge leakage through electrical conduction, and that is why it is extremely important that the active sensor element also should have as little electrical conduction as possible. The resulting irregularity of the surface could result in strong electric field inhomogeneity, the electric field exceeding the breakdown field in some places. These places could initiate an avalanche breakdown all throughout the sample. In addition, the scattering between the sputtered atoms/ions could change the incidence angle of the incoming particles to the substrate, and the normal statistical fluctuation in surface height can cause significant shadowing of the non-normal beam and eventually block some places of the substrates from any deposition, which finally leads to a porous film. A porous film can be a potential source for strong electric field concentration in certain places leading to an early breakdown of the sample. Any cavities inside the film would generate high field regions between the voids and at high concentarion of the cavity sites, theses high field regions could result in total breakdown of the sensor. A schematic representation of these poptential electrical failure mechanisms are dipected in Fig. 2 (a-c).

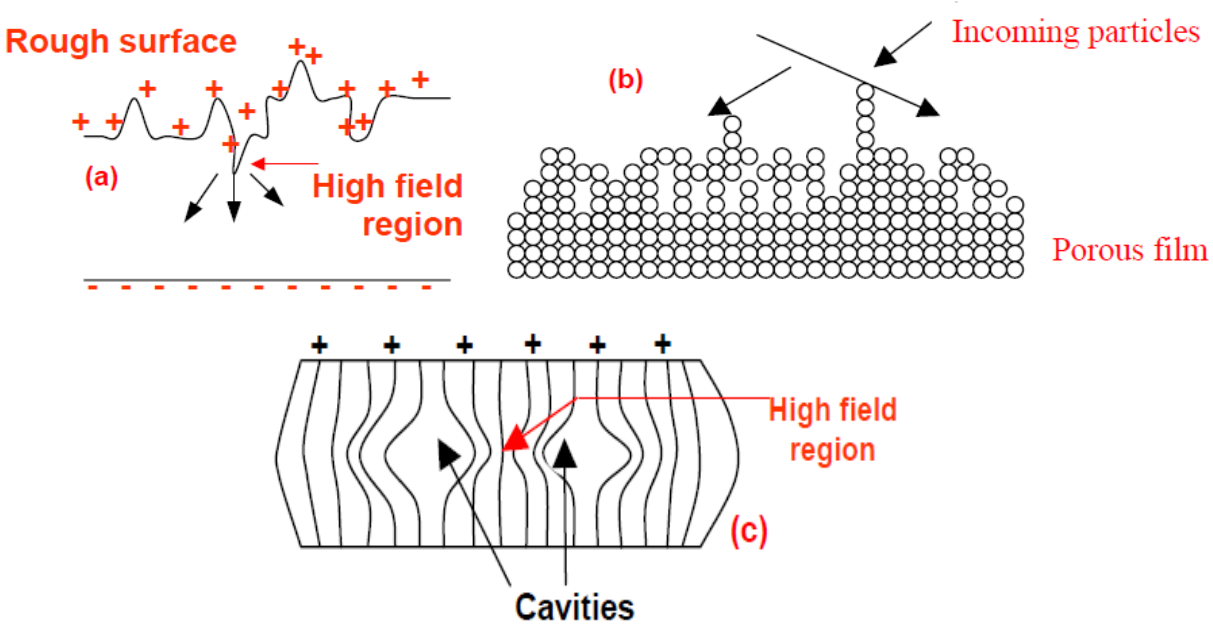

Fig. 2 (a-c): Schematic of the inhomogeneous field distribution within a film containing process induced imperfections

2. Sensor Selection Criteria

Piezoelectric materials used in the smart system must exhibit high piezoelectric constant to be able to detect small mechanical stress generated within the structure. To achieve maximum piezoelectric response, the orientation and texture of the thin film must be carefully controlled. In addition, electrical conduction through the sensor layer can act as

a source of leaking the stress-induced electrical signal through itself. Therefore, high electrical resistivity of the piezoelectric thin film sensor is essential to minimize the electrical leakage through the sensor. The chemical impurities within the film will also alter the resistivity and insulation properties of the piezoelectric films. The presence of any voids or cavities within the material would confine the electric field lines inside the high dielectric regions seperating the cavities and increasing the density of field lines in those areas thus resulting in electrical breakdown of the sensor element. With respect to temperature, the sensor components need to have high Curie temperature and being stable at elevated temperatures (e.g. up to 700°C in Al pressure die-casting). Table 1 shows the quantitative comparison of common piezoelectric materials that are possible based on the mentioned criteria.

Table 1: Comparison of piezoelectric materials [11-15]

Figure of Merits	**PZT**	***AlN***	**ZnO**	**$LiNbO_3$**
Current response: $e_{31,f}$ (C m^{-2})	-14.7	-1.0	-0.7	-5.8
Voltage response: $e_{31,f}/\varepsilon_0\varepsilon_{33}$ (GV m^{-1})	-1.2	-10.3	-7.2	N/A
Coupling Coefficient $(k_{p,f})^2$ on Si	0.2	0.11	0.06	0.02
Curie Temperature T_c (°C)	~300	~1100	N/A	1210
CTE α ($\times 10^{-6}$ K^{-1})	7.2	4	5	11
Electrical Resistivity (Ω.cm)	10^9	10^{11}-10^{16}	10^8	10^{11}

Note: CTE α ($\times 10^{-6}$ K^{-1}): 13 for H13 steel, 6 for Al_2O_3, 6.5 for TiAlN, and 10.1 for Ti.

Materials were selected based on their high temperature stability, good piezoelectric property and compatbility with the host structure. It is evident from the Table 1 that only materials with high Curie temperature such as AlN and $LiNbO_3$ would be applicable for piezoelectric measurements at elevated temperatures (e.g. up to 700°C in Al pressure die-casting). AlN has very high thermal conductivity and is a non-ferroelectric piezoelectric material with very good mechanical, thermal and chemical stability. The electrical band gap of stoichiometric AlN is very high (6.2 ev) [16], which indicates that the piezoelectric signal would prevail over the DC leakage through an extended period. AlN exhibits very high electrical resistivity (10^{16} Ω.cm) [17] which leads to its high resistance to electrical breakdown and charge leakage. Therefore, considering the combined value of high thermal stability, high Curie temperature (~1100 °C), high electrical resistivity, high thermal conductivity and good piezoelectric response, an AlN thin film is very good piezoelectric candidate to use at elevated temperatures. Being covalently bonded, this material will not introduce any ionic conduction, and due to the large band gap, the electronic conduction at high temperature will remain minimal. AlN crystallises in a hexagonal crystal structure. The Al atoms and N atoms are placed on alternate planes in a hexagonal array as shown in Fig. 3 [18].

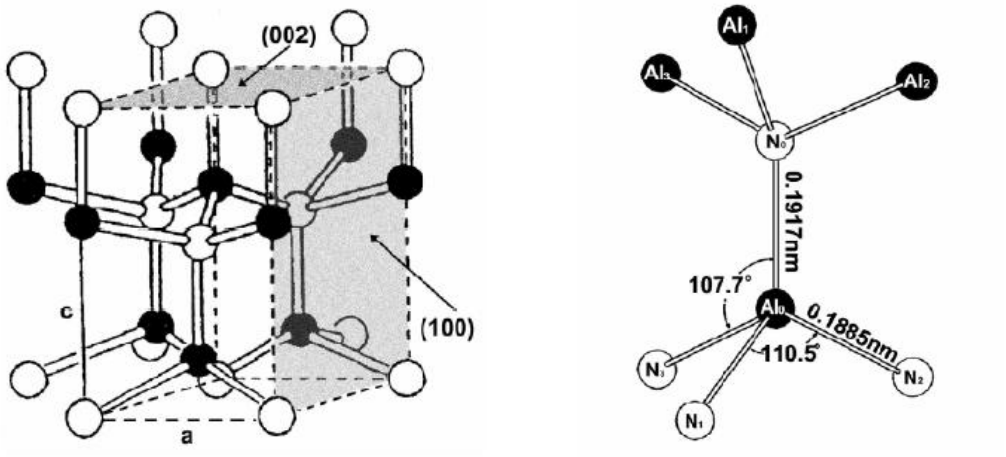

Fig. 3: Wurtzite Structure of Aluminium Nitride [18]

The piezoelectric activity in this material is found to be restricted to the perpendicular direction to the hexagonal arrays or (002) orientation, also known as the 'c'-axis. It also happens to be the natural growth direction of a thin film. The hexagonal planes have a low surface energy (probably due to the close packed geometry in which most of the chemical bonds are saturated, and there are no dangling bonds). Due to this low energy, an AlN crystal will tend to have these planes (002) exposed, which means a flake like shape will be the lowest energy configuration of an AlN crystal. The Only drawback of using AlN will be the mismatch of thermal expansion coefficient with stainless steel or tool steel substrates. The high mechanical bonding might hold on against the thermal stress developed at the interface (between the sensor element and the substrate) due to this difference. One can also place this sensor within the thermal stress-accommodating layer, which will ensure that there is no thermal stress at the interface at high temperature. The processing techniques for AlN thin film range from ion beam to reactive sputtering. Here in ACSEL (Advanced Coatings and Surface Engineering Laboratory), a closed field unbalanced magnetron sputtering system is being operated at middle frequency pulsing conditions. This closed field unbalance magnetron sputtering is a complex system where the magnets are arranged so that the magnetic field is completely closed and the unbalanced magnets would allow some of the electrons to escape the magnet's region in order to extend the plasma towards the substrate. In this study, nanocrystalline AlN thin films were sputtered from a pure metal Al target in Ar/N_2 reactive atmosphere using a Pulsed-DC closed field unbalanced magnetron sputtering (P-CFUBMS) system. The effect of working pressure and reactive gas atmosphere on orientation, intrinsic stress and piezo-response of AlN thin films is been characterized in this paper.

3. Experimental and Chracterization Techniques

AlN piezoelectric thin films were deposited on AISI 304 stainless steel coupons, (100) silicon wafers and glas substrates by pulsed closed field unbalanced magnetron sputtering system using a metal Al target (99.95%) in a gas mixture of high purity (99.999%) Ar and N_2. A cylendrical chamber equiped with four rectangular unbalanced magnetrons installed with 90-degree intervals to produce a closed magnetic field. The Al source was

powered using an Advanced Energy Pinnacle Plus Power supply which can be operated in middle frequency pulse regions. During the positive pulse period, the target volatge is reversed to 10 percent of its nominal negative sputtering voltage in order to minimize the negative charge accumilation on the target and avoid target poisening. The substrates were ultrasonically cleaned with acetone and alchohol for 15 minutes. Base pressure of 1×10^{-6} Torr was achieved before thin film deposition and then the substrates were etched by Ar^{+} ions with a bias of -400 volts to remove the surface contaminations. The Cr layer was deposited as the bottom and a top electrode, which also acts as adhesion layer in our coating system.

The crystal structure of the films was characterized by monochromatic Cu-K_{α} radiation on a Philips X-ray diffractometer model PW1729 operated at 45kV and 30 mA. The AlN film texture was analyzed using XRD Rocking Curve method with a Simens X-ray diffractometer (model KRISTALLOFLEX-810). The composition and bonding nature of these films were analyzed by high-resolution x-ray photoelectron spectroscopy (XPS). The dynamic oxidation studies of AlN films were carried out in the differential scanning calorimetry (DSC) in which the AlN film deposited on a Si wafer was placed in the alumina crucible and were heated from room temperature to 1400 °C in flowing argon (55 sccm) using a heating rate of 20 Kmin-1. An empty pure alumina crucible served as an inert reference. After the DSC tests, XRD measurements of the annealed films were carried out on a Philips X-ray diffractometer in the $\theta/2\theta$ geometry using Cu Kα radiation (20 kV and 30 mA) on order to investigate the phase transformations and structure evolution durin heating procedure.

Direct piezoelectric response of AlN thin films were measured by Lock-in amplifier. An actuator was placed in contact with the top surface of our system, which applies cyclic load to the AlN thin film. The actuation frequency and amplitude are controlled using a function generator. As we increase the amplitude of the actuation, the amount of force on the film is increased linearly. The travel distance of the actuator is a function of voltage applied to it and when we have the actuator in contact with the film, the increase in displacement would generate more loads on the film. The schematic of this design is shown in Fig 4.

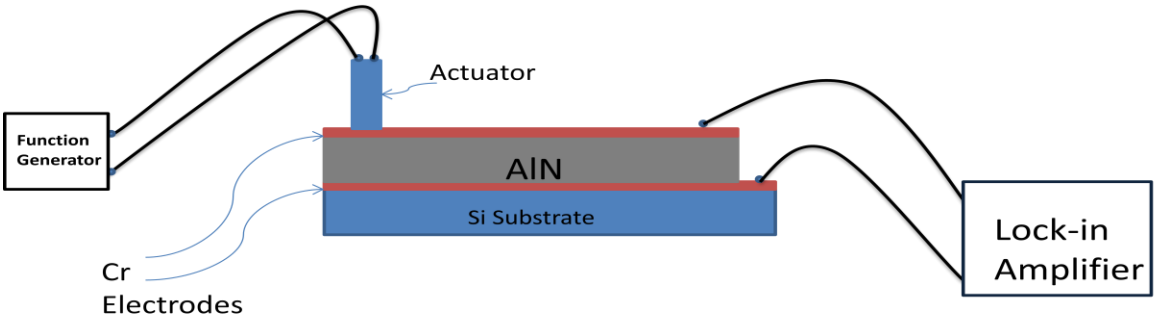

Fig. 4: Schematic of our direct piezoelectric measurements setup using an actuator, this is derived by a function generator and uses the lock-in amplifier to measure the piezo-voltage output.

4. Results and Disscusion

As mentioned in the previous section, to obtain the maximum piezoelectric effect in the coating sensor, the orientation of the AlN thin film must be controlled to produce (002) oriented thin film structures. Another factor that governs the thin film quality is the

amount of intrinsic stress presented within the film and its interface. A thin film with minimal amount of stress is desired to avoid any film delamination during operation. AlN thin films with different working pressure were deposited using P-CFUBMS system and their residual stress, crystall size and orientation/texture were examined using XRD and rocking curves. When varying the working pressure during the deposition we are not only altering the amount of reactive gas present, we also alter the volatility conditions within the chamber. When the pressure is increased, it allows for more frequent ion bombardment on the substrate yet with less velocity. Too low of a working pressure can lead to very slow deposition rates, introduction of high energetic ions approcahing substrate due to less collision, and possibly not allow the plasma to ignite. The films were deposited varing working pressure from 2 mtorr upto 6.5 mtorr to investigate the effect of working pressure alteration on residual stress, crystall size and orientation of the AlN thin films, as depicted in Fig. 5.

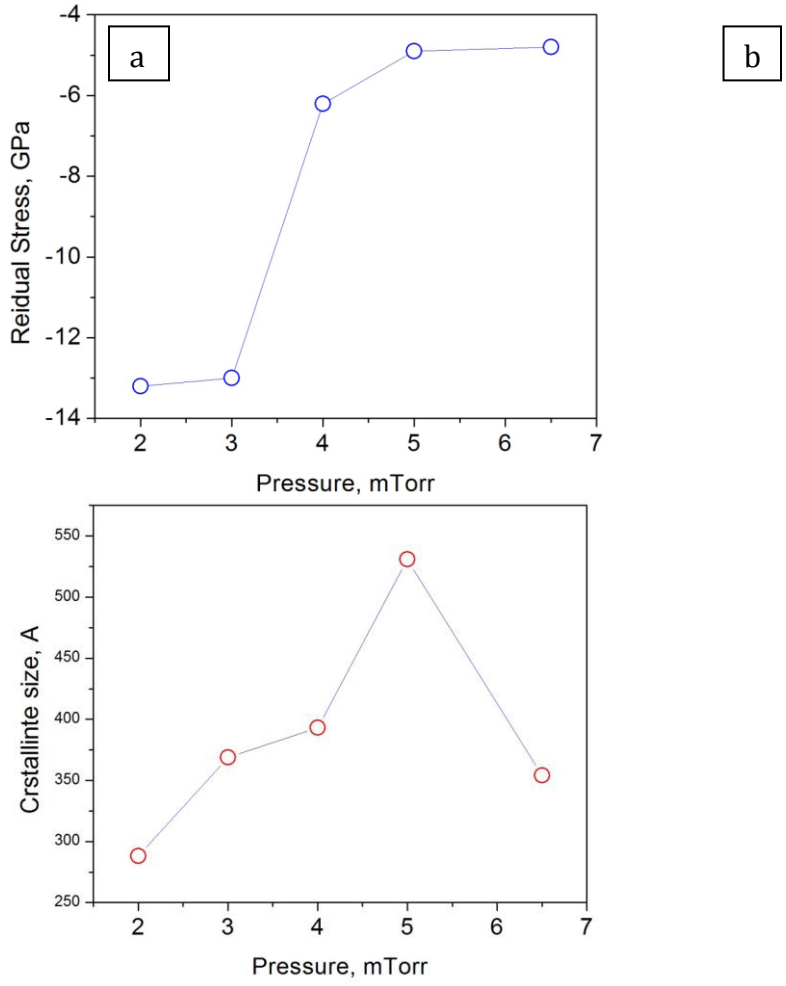

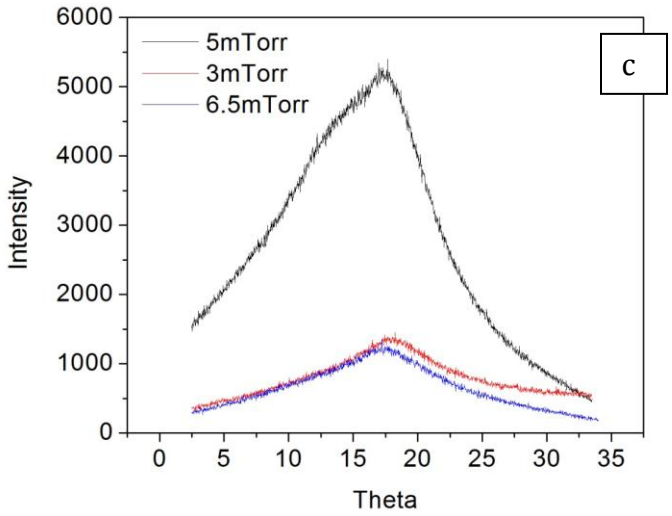

Fig. 5: Relation between working pressure, residual stress (a) and crystalline size (b). Rocking curves for different working pressure conditions (c).

As the working pressure increases inside the chamber, more ion collisions occur and ions will loose their energy upon collision. At higher working pressures, the amount of ion bombardment on the substrate decreases due to the arival of low energy ions thus producing films with fewer defects and with lower comperasive stress level. In contrary, at lower working pressures, collision frequency of ions is much lower and ions with high energy will impact the substrate introducing more defects and higher compressive stress level. The size increases with the rising of pressure and arrives at the maximum at 5 mTorr, as depicted in Fig. 5 (b). Then it drops off at 6.5 mTorr. The maximum crystallite size at 5mTorr is consistent with our previous results where the films deposited at 5mTorr exhibit approximately 99% (002) orientation. Higher textured (002) growth produces larger crystallite size. The film deposited at 5mTorr also demonstrates a lower residual stress, as shown in Fig. 5 (a) and (c). The narrower and more intense rocking curve, indicates the presence of lower residual stress and stronger (002) orientation. Thus, the film at 5 mtorr working pressure shows the lowest residual stress, larger crystall size and higher texturing in preffered (002) orientation.

In order to test the stability of AlN thin films at higher temperature, DSC method was used to investigate thermal stability, as Shown in Fig.6 (a), and then films were analyzed by XRD to evaluate any phase change, as depicted in Fig. 6 (b) [10].

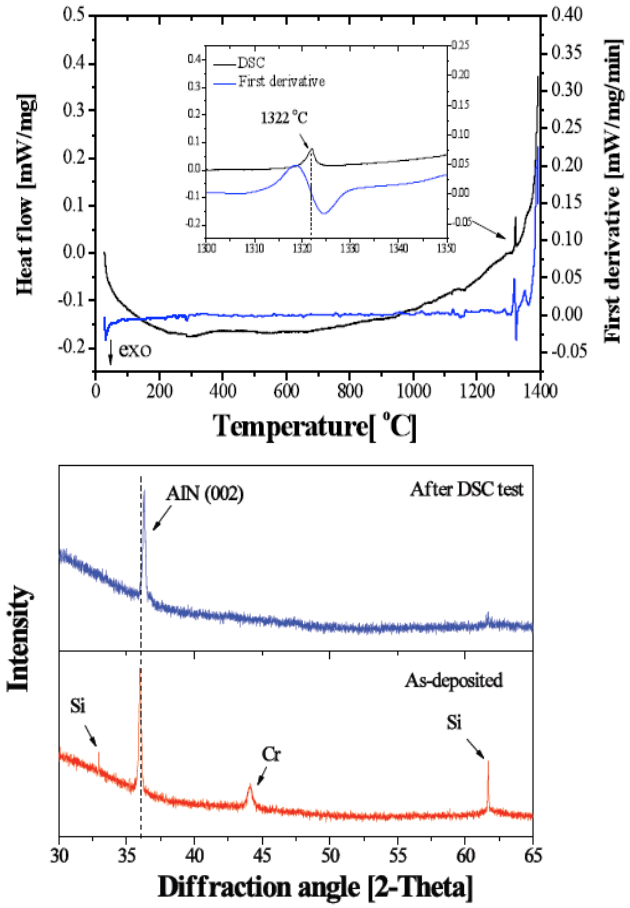

Fig. 6: (a) DSC curve and first derivative obtained at 20 K/min heating rate in the flowing argon (55 sccm) and (b) its corresponding XRD graph before and after DSC analysis.

AlN thin film with Cr electrode deposited on silicon substrate was heated from room temperature upto 1400 °C with heating rate of 20 K/min in a flowing argon (55 sccm) environment. The DSC curve indicates that there was no apparent phase change below 1322 °C, confirming the supperior thermal stability of AlN films. An endothermic peak at 1322 °C suggests the formation of Cr-Si compound since this temperature is very close to Si melting temperature. A comparison of XRD graphs of as-deposited film with the same film after DSC annealing at 1400 °C, will identify any crystal phase change during DSC analysis. The silicon and Cr peaks are disappeared after DSC test, as shown in Fig. 6 (b), indicating the partial melting of silicon substrate and thus the formation of Cr-Si compound. However, one can see that the peak for AlN (002) orientation is not altered after DSC test compare to as-deposited film, which indicates the excellent structural stability of AlN films upon heating.

XPS analysis was performed to identify the composition of AlN films and its bonding nature. Fig. 7 (a, b) shows the Al 2p and N 1s core level peaks of the samples deposited at 20/80 (CFAlN 19), 40/60 (CFAlN 20), 80/20 (CFAlN 21) and 100 (CFAlN 22) nitrogen/argon ratio. Etching by Ar^+ ions was used to remove all the contaminant; but even after this ion sputtering, oxygen peak still presented in the films which could be diffused into the film deeply. Fig. 7 (a) and (b) show the Al 2p and N 1s peaks at 73.5 eV and 396.5 eV, respectively. The 73.5 eV and 396.5 eV binding energies are assigned to

Al-N and N-Al bonding, acording to XPS reference book, respectively. There are no shoulder peaks, such as Al-O peak at 75 eV or Al-Al peak at 72 eV, in Al 2p spectra that is the indication that aluminium atoms are only bonded to nitrogen atoms and aluminium oxide or metallic aluminium is not presented in these films. Another important information that one can get from XPS, is the composition of the film that could be calculated by the integration of the area under the peaks. Table 2 shows the atomic concentartions of various elements present in the film and calculates the Al/N atomic ratio to confirm the formation of stoichiometry AlN thin films.

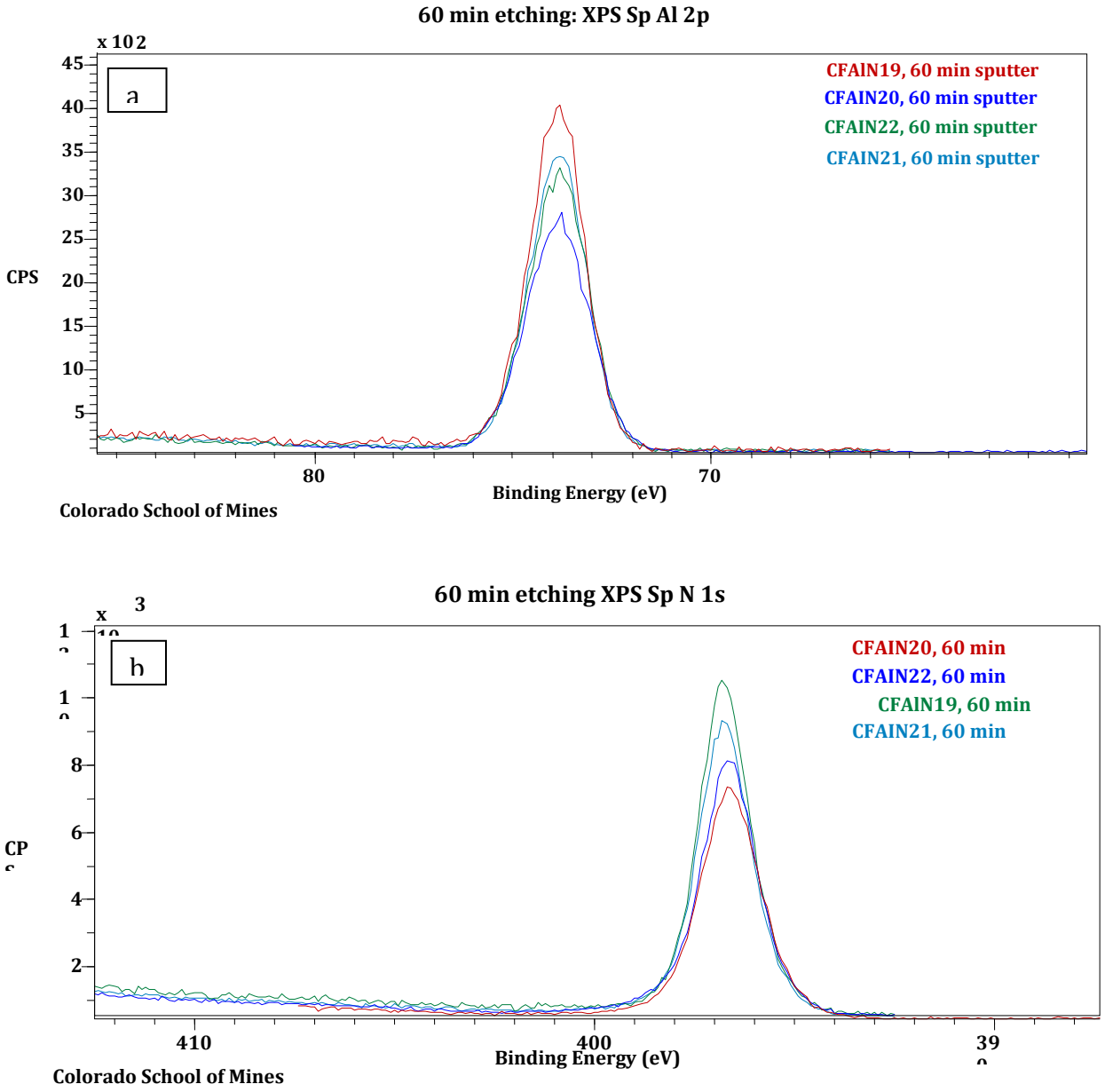

Fig. 7: (a) Al 2p and (b) N 1s core level profiles after one hour etching by argon ions from the same samples with different gas ratio.

Table 2: Composition and atomic concentration of tested films by XPS and their Al/N atomic ratio after one hour etching with Ar ions.

Sample Name	*% Atomic Conc. (O 1s)*	*% Atomic Conc. (Al 2p)*	*% Atomic Conc. (N 1s)*	*Al/N Atomic Ratio*
CFAlN 19 (20/80, N_2/Ar ratio)	12.04	39.42	48.53	**0.81**
CFAlN 20 (40/60, N_2/Ar ratio)	7.32	48.04	44.04	**1.09**
CFAlN 21 (80/20, N_2/Ar ratio)	6.46	48.33	44.52	**1.08**
CFAlN 22 (100/0, N_2/Ar ratio)	10.58	46.46	41.15	**1.12**

The Al/N atomic ratio for sample with 20 percent nitrogen gas ratio was not close to one which indicates that stoichiometric AlN was not formed with that deposition parameters; but any other film with higher nitrogen/argon gas ratio (>20/80, nitrogen/argon ratio), will produce stoichiometric AlN films. The amount of oxygen presented in these films is not reacted with Al since there was no evident peak for Al-O formation, thus the oxygen is probably difussed in the film after the exposure of the films in air.

The preliminary piezo-response of two different AlN thin films are measured and compared, as illustrated in Fig. 8. The film that was deposited at 80% nitrogen to argon ratio, showed about 3-4 times higher piezo-response compared to the one deposited at 20% nitrogen/argon ratio. This result is in a good agreement with our XPS result that the film at 20% nitrogen/argon ratio is not stoichiometric AlN and thus its piezo-response is smaller than the film at 80% nitrogen/argon ratio, which is stoichiometric AlN. There is another interesting point present here, which is the linear correlation between the applied force and output piezo-response. This is in agreements with literature results and constitutive equations describing mechanical-electrical domains and their conversions.

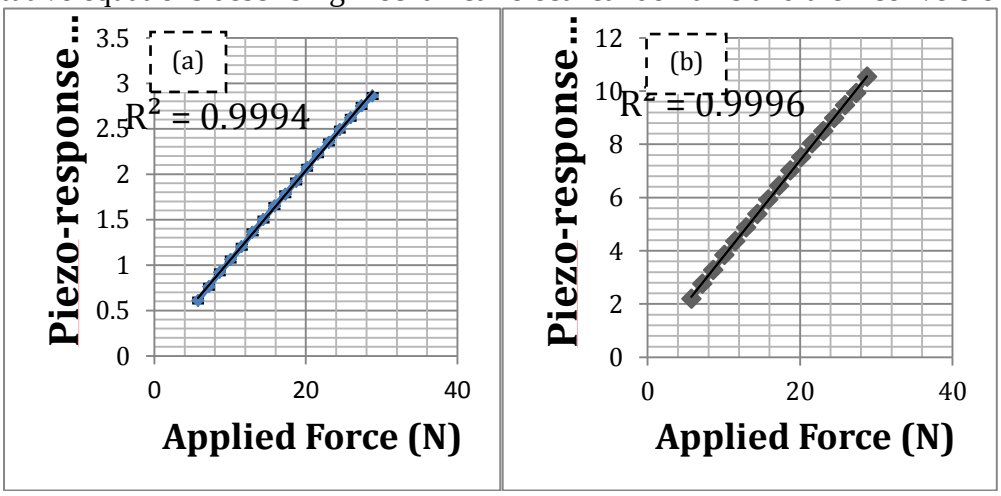

Fig 8: Piezo-response of: (a) AlN thin film deposited at 5mtorr of working pressure, 1kW of power, 1.0 micro- second of reverse time and 20% of nitrogen/argon ratio. (b) AlN thin film deposited at 5mtorr of working pressure, 1kW of power, 1.0 microsecond of reverse time and 80% of nitrogen/argon ratio.

5. Accomplishments

A 'Smart' die coating based on thin film piezoelectric sensor embedded within a tribological coating system has been designed. AlN was selected as a sensor material due to its high thermal stability and good piezoelectic properties compared to other candidates. AlN thin films with strong (002) orientation were deposited by pulsed closed

field unbalanced magnetron sputtering system. The effect of working pressure on orientation, residual stress and crystalline size of AlN films were investigated. It has been found that the films with high working pressure have less residual stress but at very high working pressures, defects such as prosity are introduced. At low working pressure, AlN film exhibited high amount of residual stress and the working pressure of 5 mtorr was found to be optimum to achive highly textured (above 99% (002)orientation) and low residual stress AlN films. The XPS result showed that the films are in nitride forms and no evident oxides or carbides have formed inside the films. The new piezo-measurement technique is a promising method to evaluate piezo-output of AlN film in various deposition conditions.

6. References

[1] Mayrhofer P.H., Mitterer C., Hultman L.,and Clemens H. "Microstructural design of hard coatings", Progress in Materials Science, vol 51, No. 8, pp1032-1114 (2006).

[2] Lin, J., Carrera, S., Kunrath, A.O., Zhong, D., Myers, S., Mishra, B., Ried, P., and Moore J.J.., "Design Methodology for Optimized Die Coatings: The Case for Aluminum Pressure Die-Casting, (Invited paper B7-1-1, ICMCTF, presented Monday May 2nd, 2005, San Diego), Surface and Coatings Technology, vol 201, pp 2930–2941 (2006).

[3] Lin, J., Myers, S., Mishra, B., Moore, J.J., and Ried, P., "Optimization of a Graded, Multilayer Die Coating System for Use in Al Pressure Die Casting", 111th Metalcasting Congress, Huston, May, (2007).

[4] Lin, J., Myers, S., Mishra, B., Moore, J.J., and Ried, P., "An examination of Coating Architecture in the Development of an Optimized Die Coating System for Aluminum Pressure Die Casting", 112th Metalcasting Congress, Atlanta, May, (2008).

[5] L.Yin, X.-M. Wang and Y.-P. Shen, "Damage-monitoring in composite laminates by piezoelectric films"**,** *Computers & Structures***, 59**(4): 623, (1996).

[6] Hisao Fukunaga, Ning Hu and Fu-Kuo Chang, "Structural damage identification using piezoelectric sensors", *International Journal of Solids and Structures*, **39**(2): 393, (2002).

[7] W.K. Chiu, "Damage monitoring in metallic structures using piezoelectric thin film sensors", *Polymers & Polymer Composites*, **5**(2): 121, (1997).

[8] W.K. Chiu, S.C. Galea, H. Zhang, R. Jones, Y.C. Lam, "Use of piezoelectric thin film sensors for structural integrity monitoring", *Journal of Intelligent Material Systems and Structures*, **5**(5): 683, (1994).

[9] Z. M. Xiao, J. Bai and R. Maeda, "Electro-elastic stress analysis on piezoelectric inhomogeneity-crack interaction", *International Journal of Solids and Structures*, **38**(8): 1369, (2001).

[10] Lin, J.,Wang, F., Bhattacharyya, S., Hasheminiasari, M., Myers, S., Mishra, B., Moore, J.J., and Ried, P., "Development of a 'Smart' Die Coating for Al Pressure Die Casting", 113th Metalcasting Congress, Nevada, April, (2009).

[11] Muralt P., Ferroelectric thin films for micro-sensors and actuators: a review, *J. Micromech. Microeng.*, vol **10**, pp136, (2000).
[12] Moulson A.J., and Herbert J.M., Electroceramics, Chapman and Hall, London, (1990).
[13] Gregory O.J., Slot A.B., Amons P.S. and Crisman E.E., High temperature strain gages based on reactively sputtered AlNx thin films, *Surface and Coatings Technology*, vol **88**, pp 79, (1996).
[14] Barker A., Crowther S., and Rees D., Room-temperature r.f. magnetron sputtered ZnO for electromechanical devices, *Sensors and Actuators A*, vol **58**, pp 229, (1997).
[15] Tomar M., Gupta V., Mansingh A. and Sreenivas K., Temperature Stability of c-axis Oriented LiNbO3/SiO2/Si Thin Film Layered Structures, *J. Phys. D: Appl. Phys.*, vol **34**, No. 15, pp 2267, (2001).
[16] Joo H.Y. and Kim H.J., Spectrophotometric Analysis of Aluminum Nitride Thin Films, *Journal of Vacuum Science and Technology. A.*, vol **17**, No. 3, pp 862 (1999).
[17] Tsubouchi, K. & Mikoshiba, N., Zero temperature coefficient saw delay line on A1N epitaxial films 1983 Ultrasonics Symposium, Proc. IEEE, New York. USA, pp. 299-310 (1980).
[18] Xu, Xia-Hong, Xi'an, Morphological properties of AlN piezoelectric thin films deposited by DC reactive magnetron sputtering, *Thin Solid Films*, Vol. **388** (2000).

2. CATALYST ENGINEERING USING SURFACE-DOPANT MODIFICATION

Ryan O'Hayre[1], Yingke Zhou[1], Robert Pasquarelli[1], Tim Holme[2], Joe Berry[3], and David Ginley[3]

[1] Colorado School of Mines, Dept. of Metallurgical and Materials Engineering, Golden, CO. USA
[2] Stanford University, Dept of Mechanical Engineering, Stanford. CA. USA
[3] National Renewable Energy Laboratory, Golden, CO. USA

Abstract

This research project examines the emerging potential of "smart surface functionalization" using nitrogen doping to enhance catalysis for direct methanol fuel cells. We have found clear and compelling experimental evidence that catalytic activity of a variety of low-temperature fuel-cell relevant reactions is significantly enhanced when a nitrogen-functionalized carbon support is used in place of a standard carbon support. This level of enhancement brings the technological promise of low-temperature fuel cells much closer to reality. Furthermore, the basic idea of catalyst support surface-dopant functionalization opens the door to a game-changing new method for catalyst design, with applications not only in fuel cells, but also in industrial chemistry, biology, energy, and even medicine. While the reason for this surprising dopant-induced enhancement effect have before been uncertain, our research has produced both experimental and theoretical results that clarify the situation by using highly ordered

pyrolytic graphite (HOPG) as a model support. Our experimental evidence and theoretical calculations show that the activity enhancement is due to a chemical doping effect, where N-HOPG donates charge to Pt catalyst clusters, changing the d-band electronic structure, and therefore the catalytic activity. Our theoretical calculations suggest that B-doping at low levels will have a similar impact as high-doses of N-doping. Therefore, a predictive model has been proposed, and experimental confirmation is ongoing.

Accomplishments for Reporting Period

Our recent findings are detailed in several recently published scientific papers [1-3]. A brief summary of our recent work is provided below:

- Geometrically well defined Pt/HOPG model catalyst systems have been successfully developed and have proven to be a uniquely powerful platform to investigate the effects of N-doping.

- Using SEM and AFM imaging, combined with statistical image analysis methods, the structural effects of N-doping have been quantified. By favoring nucleation over growth during the Pt electrochemical deposition process, N-doping leads to significantly smaller average Pt particle size (by approximately a factor of two) and a narrower Pt particle size distribution. Furthermore, N-doping significantly reduces Pt particle agglomeration, as measured by statistical nearest neighbor analysis.

- Using electrochemical techniques (IV, CV, EIS), the catalytic effects of N-doping have been quantified. N-doping leads to substantial catalytic enhancements (up to 10-fold on a Pt-mass normalized basis) for both MOR and ORR activity.

- Based on a careful analysis of structural versus catalytic effects, we have been able to conclude that catalytic enhancement due to N-doping can only be partially explained by improved Pt utilization due to decreased Pt particle size. (Decreased Pt particle size accounts for about ½ of the observed mass-normalized enhancement effect.) The remainder of the enhancement effect appears to be due to a dopant-induced increase in *intrinsic* catalytic activity. *This is a significant conclusion, because it suggests that N-doping can be used to intrinsically boost the performance of Pt catalysts.* In contrast, Ar-doped control samples do not show this intrinsic catalyst activity enhancement effect, suggesting this effect may be specific to nitrogen doping.

- N-doping improves the degradation resistance of the Pt-catalyst system (by at least a factor of ten) during MOR cycling (as measured by final vs. initial peak CV currents obtained from N-doped and undoped HOPG/Pt systems after 10,000 cycles). In contrast, Ar-doping does not provide any degradation resistance (and may in-fact accelerate degradation).

- *The above findings are significant, because they show that only N-doping provides increased agglomeration resistance and significantly enhanced intrinsic catalyst activity.* These key observations clearly indicate that N-doping provides a significant chemical influence that is not present in the Ar-doped sample. We suggest that N-doping imparts a *significant intrinsic chemical interaction effect* which enhances the overlying Pt nanoparticle activity and stability. In contrast, the mostly physical defects generated by the Ar-implantation process promote decreased *initial* Pt particle size but do not enhance catalytic activity or stability.

- DFT based modeling efforts (in collaboration with Stanford University) indicate that the catalytic activity enhancement from N-doping is due to a chemical doping effect, where N-HOPG donates charge to Pt clusters, changing the d-band electronic structure, and therefore the catalytic activity.

- A facilities usage award has recently been granted by the Oak Ridge National Laboratory (ORNL) National Microscopy User's Facility to image the structural and chemical effects of N-doping at atomic-level. Direct atomic-level visualization of N-doping effects in Pt/C fuel cells would likely warrant immediate high-impact publication.

- An effort is now underway to apply these same investigative techniques to PtRu catalyst systems and to other dopants, such as CF_4, sulfur, iodine and boron. *Proof that these interactions are extendable to a variety of catalytic systems would potentially open the door to game-changing new methods for catalyst design.*

In summary, the major goals and tasks associated with quantifying the N-doping effect in Pt/C fuel cells have been successfully accomplished. Our efforts are now focused on developing a deep understanding of the fundamental mechanisms underlying the N-doping effect, and then exploring whether these impressive catalytic enhancements can be achieved with other dopants and/or other catalyst systems.

REFERENCES

[1] Y. Zhou, R. Pasquarelli, T. Holme, J. Berry, T. Ohno, D. Ginley, R. O'Hayre, "Dopant-induced electronic structure modification of HOPG surfaces: implications for high activity fuel cell catalysts *Journal of Physical Chemistry C*, **114**, 506-515 (2010)
[2] Y. Zhou, R. Pasquarelli, T. Holme, J. Berry, D. Ginley, R. O'Hayre, "Improving PEM Fuel Cell Catalyst Activity and Durability Using Nitrogen-Doped Carbon Supports", Cover Feature—*Journal of Materials Chemistry*,**16**(42), 7830-7838, (2009)
[3] T. Holme, Y. Zhou, R. Pasquarelli, R. O'Hayre, "First principles study of doped carbon supports for enhanced platinum catalysts", accepted, *Phys. Chem. Chem. Phys*.

3. STIMULI-RESPONSIVE POLYMER BRUSHES FOR SMART SURFACES AND INTERFACES

Daniel Knauss, David Wu, and Stephen Boyes, department of Chemistry and Geochemistry, Colorado School of Mines

Abstract
The objective of this part of the research is to gain a fundamental understanding of polymer brush surfaces and other functionalized interfaces and to design stimulus-response behavior. The potential properties include switching behavior in response to external forces, and controlled adhesion leading to improved tribological properties and applications in micro/nanoelectromechanical devices, chemical separations, and functional coatings. This project will systematically investigate the effect of the composition, density, thickness and architecture of polymer brushes on the nanomechanical properties and tribological performance of the films on a variety of different substrates. The project will involve aspects of theory combined with synthesis and design elements allowing for the determination of a fundamental understanding and the development of improved materials.

Approach
Theory
A new scaling theory was developed toward understanding the interfacial behavior of block copolymer brushes. This theory identifies a new *stretched interface* regime for the interfacial width, w, in diblock copolymer brushes at high grafting densities or low values of the Flory interaction parameter, χ. Here, the width scales as $w \sim \chi^{-1}$ as opposed to the Helfand-Tagami expression $w \sim \chi^{-1/2}$ for free block copolymers and immiscible polymer blends. The scaling theory is in qualitative agreement with experimental neutron reflectivity (NR) and grazing incidence small angle X-ray scattering (GISAXS) measurements by collaborators at the University at Akron, and our numerical self-consistent field (SCF) calculations on the internal structure of as-deposited high grafting density (0.6 chains/nm^2) ultrathin ($d < 25$ nm) diblock copolymer brushes formed from polystyrene and poly(methyl acrylate) blocks.

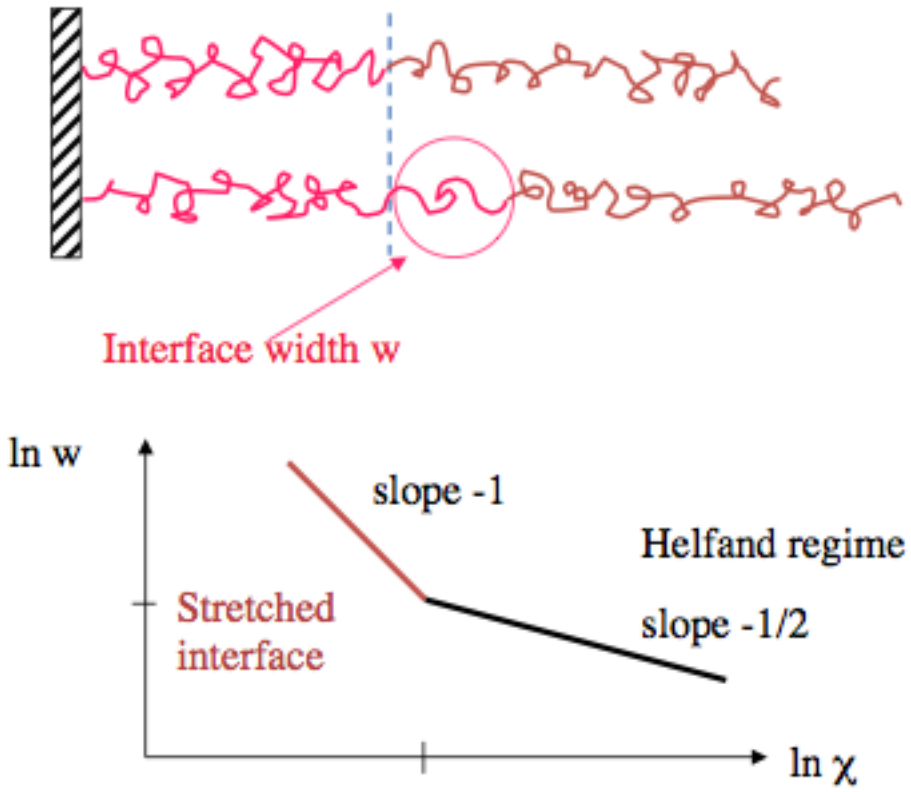

Figure 1. Relationship of the interfacial width relative to c for block copolymer brushes

Synthesis

Polymer brushes have been prepared on a variety of different substrates using controlled polymerization techniques including reversible addition fragmentation chain transfer (RAFT) polymerization and atom transfer radical polymerization (ATRP). These living radical polymerization (LPR) techniques have allowed the preparation of polymer brushes with unique structural functionality, unobtainable by other techniques, via the use of highly functional ("smart") monomers or end-group functionalization that facilitate the preparation of polymer brushes with stimuli-responsive tribological properties, controlled wetting and dewetting behavior, self-cleaning properties, and controlled adhesion. To achieve the overall objective of producing polymer brushes with controllable tribological, adhesive, and other surface properties, a number of smaller technical objectives have been accomplished, these include:

1. Theoretical understanding of the switching behavior of stimuli-responsive brushes
2. Modification of a variety of substrates by attachment of initiating systems including RAFT agents and ATRP initiators
3. Development of living polymerization techniques from modified surfaces
4. Design and synthesis of stimuli responsive polymer brush architectures using suitable functional monomers and polymer chain compositions
5. Establish conditions for the systematic variation of the thickness, density, architecture and composition of the polymer brushes

6. Evaluation of polymer brush properties that produce optimum tribological and adhesion performance.

Accomplishments

Several significant findings have been obtained and have been communicated to the scientific community. Key findings include:

- Scaling of the interfacial region width relative to c in diblock brushes has been defined.
- Our theory and the comparison with experiments were published in *Macromolecules* (Akgun et al., *Macromolecules* 2009, 42, 8411-8422).
- The synthesis of surface initiated stimuli responsive diblock copolymer brushes was published in (Rowe, et al., Macromolecules 2008, 41, 4147-4157).
- Developed a new technique for the preparation of stimuli responsive diblock copolymer brushes using a combination of ATRP and RAFT polymerization.
- Demonstrated that the conversion of macro-ATRP initiators to macro-RAFT agents can be achieved using either Cu(0) or tin (II) 2-ethylhexanoate.
- Using the above procedures, diblock copolymers of poly(acrylic acid) (PAA) were for the first time prepared without the use of deprotecting chemistry.
- The prepared diblock copolymer brushes demonstrated stimuli responsiveness after treatment with different quality solvents.
- Poly(methyl acrylate) brushes with quaternary ammonium functionalized chain ends have been produced.
- Poly(2-ethyloxazoline) brushes grown from silicon wafers have been produced for the first time.

The new technique developed for the preparation of diblock copolymer brushes using a combination of ATRP and RAFT polymerization is shown below. Conversion of bromine end groups of homopolymer brushes prepared by ATRP via a modified atom transfer addition reaction to a RAFT agent and diblock extension via RAFT polymerization allowed for the direct formation of well defined stimuli responsive diblock copolymer brushes.

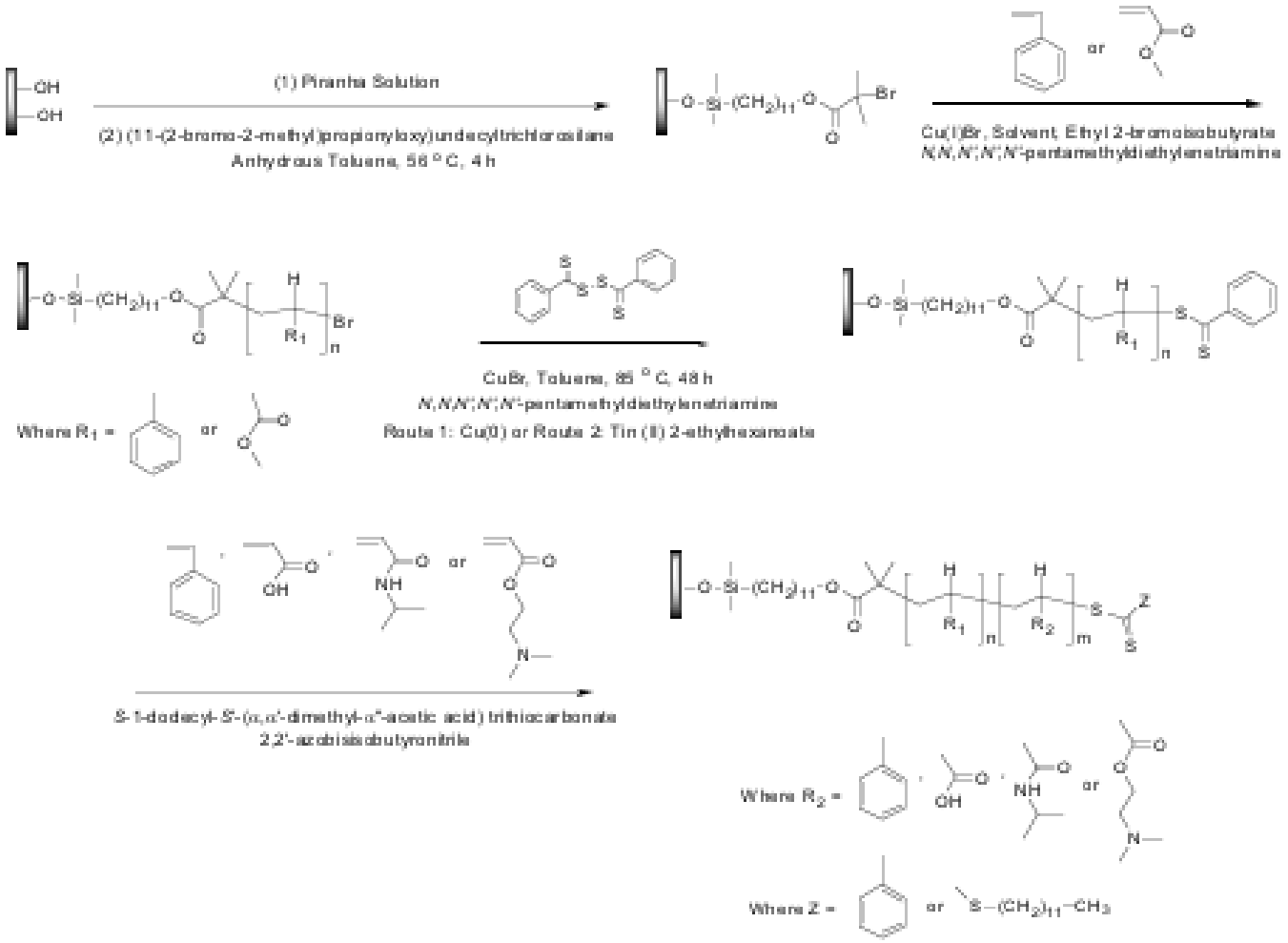

Figure 2. General route of formation of stimuli-responsive, diblock copolymer brushes through a combination of both ATRP and RAFT polymerization techniques.